ORIGINAL CLINICAL RESEARCH REPORT

OPEN

A Novel 3-Dimensional Printing Fabrication Approach for the Production of Pediatric Airway Models

Andrew D. Weatherall, BMed,*† Matthew D. Rogerson, BSc Hons,‡ Michelle R. Quayle, BSc Hons,‡ Michael G. Cooper, MBBS,* Paul G. McMenamin, PhD,‡ and Justin W. Adams, PhD‡

BACKGROUND: Pediatric airway models currently available for use in education or simulation do not replicate anatomy or tissue responses to procedures. Emphasis on mass production with sturdy but homogeneous materials and low-fidelity casting techniques diminishes these models' abilities to realistically represent the unique characteristics of the pediatric airway, particularly in the infant and younger age ranges. Newer fabrication technologies, including 3-dimensional (3D) printing and castable tissue-like silicones, open new approaches to the simulation of pediatric airways with greater anatomical fidelity and utility for procedure training.
METHODS: After ethics approval, available/archived computerized tomography data sets of patients under the age of 2 years were reviewed to identify those suitable for designing new models. A single 21-month-old subject was selected for 3D reconstruction. Manual thresholding was then performed to produce 3D models of selected regions and tissue types within the dataset, which were either directly 3D-printed or later cast in 3D-printed molds with a variety of tissue-like silicones. A series of testing mannequins derived using this multimodal approach were then further refined following direct clinician feedback to develop a series of pediatric airway model prototypes.
RESULTS: The initial prototype consisted of separate skeletal (skull, mandible, vertebrae) and soft-tissue (nasal mucosa, pharynx, larynx, gingivae, tongue, functional temporomandibular joint [TMJ] "sleeve," skin) modules. The first iterations of these modules were generated using both single-material and multimaterial 3D printing techniques to achieve the haptic properties of real human tissues. After direct clinical feedback, subsequent prototypes relied on a combination of 3D printing for osseous elements and casting of soft-tissue components from 3D-printed molds, which refined the haptic properties of the nasal, oropharyngeal, laryngeal, and airway tissues, and improved the range of movement required for airway management procedures. This approach of modification based on clinical feedback resulted in superior functional performance.
CONCLUSIONS: Our hybrid manufacturing approach, merging 3D-printed components and 3D-printed molds for silicone casting, allows a more accurate representation of both the anatomy and functional characteristics of the pediatric airway for model production. Further, it allows for the direct translation of anatomy derived from real patient medical imaging into a functional airway management simulator, and our modular design allows for modification of individual elements to easily vary anatomical configurations, haptic qualities of components or exchange components to replicate pathology. (Anesth Analg 2021;133:1251–9)

KEY POINTS

- **Question:** Can 3-dimensional (3D)-printing technology be combined with patient-derived medical imaging datasets to produce anatomically and haptically accurate pediatric airway management simulators?
- **Findings:** A combination of direct 3D-printing and materials casting in 3D-printed molds has produced a functional simulator that replicates the anatomy of a 21-month-old patient in a manner with utility for training in pediatric airway management in a 21-month-old patient.
- **Meaning:** Commercially available technology can now be coupled with standard clinical imaging datasets to produce high fidelity airway management training devices that are designed to allow for rapid modification and customization to suit specific clinical demands and simulate the difficult pediatric airway.

From the *Department of Anaesthesia, The Children's Hospital at Westmead, Sydney, Australia; †Discipline of Child and Adolescent Health, The University of Sydney, Australia; and ‡Centre for Human Anatomy Education, Department of Anatomy and Developmental Biology, Monash University, Melbourne, Australia.

DOI: 10.1213/ANE.0000000000005260

Accepted for publication September 18, 2020.

Funding: None.

The authors declare no conflicts of interest.

Supplemental digital content is available for this article. Direct URL citations appear in the printed text and are provided in the HTML and PDF versions of this article on the journal's website (www.anesthesia-analgesia.org).

Reprints will not be available from the authors.

Address correspondence to Andrew D. Weatherall, BMed, Department of Anaesthesia, The Children's Hospital at Westmead, Sydney 2145, Australia. Address e-mail to andrew.weatherall@health.nsw.gov.au.

GLOSSARY

3D = 3-dimensional; **ABS** = acrylonitrile butadiene styrene; **CHAE** = Centre for Human Anatomy Education; **CT** = computerized tomography; **HU** = Hounsfield unit; **MASSIVE** = Multi-modal Australian Sciences Imaging and Visualisation Environment; **MRI** = magnetic resonance imaging; **SLA** = stereolithography; **TMJ** = temporomandibular joint; **UV** = ultraviolet

Airway management is a key technical skill in pediatric critical care with potentially significant complications.[1–6] This is particularly the case for infants, those weighing less than 10 kg and those in whom multiple airway interventions are required.[1,4] In infants, there are unique anatomical and functional airway characteristics that contribute to these challenges, which are compounded by the continuous changes in airway morphology during development before its adult configuration is achieved between the ages of 6 and 8 years.[7–9]

Developing airway management skills during training has traditionally utilized models.[10] However, many pediatric airway models fail to adequately reflect the anatomical differences between young children and adults, and commonly demonstrate inaccurate anatomy, excessive morphological variation between pediatric and neonatal models, deficiencies of haptic qualities, and difficulties inculcating correct procedural techniques in simulated tasks.[11–13]

This is not surprising. Current models generally attempt to replicate a single "idealized" morphology, rather than encompassing variance. With the exception of condition-specific models, such as Pierre-Robin models, conditions with associated airway pathology are not reflected in most mannequins, even though many specific conditions or syndromes are associated with much higher rates of airway management difficulty.[14]

Contemporary models are also limited in their anatomical accuracy by the quality and detail of the molds used in their creation, in part, due to the accuracy of the data used to develop them. Additive manufacturing techniques (broadly termed 3-dimensional [3D] printing) now provide the opportunity to improve pediatric airway models by integrating computerized tomography (CT) and magnetic resonance imaging (MRI) data with 3D computer-assisted design to generate highly accurate anatomical representations. The impact of 3D design and printing has already been demonstrated in the production of educational anatomical models for undergraduate and postgraduate levels, anesthesia practitioners, and in preoperative planning.[15–18]

We present a novel application of 3D-printing technology to the production of a pediatric mannequin, which aims to replicate the internal and surface anatomy of the pediatric airway to a high degree of accuracy, and which can be used to demonstrate airway management techniques, including surgical interventions. Additionally, we present 3D printing and casting methods underlying the construction of a pediatric simulator integrating a range of tissue types, including bones, mucosa, muscles, and cartilage with haptically and mechanically appropriate materials. Finally, we discuss current and future applications of our methods, including modularity, which should enhance their use in clinical training.

METHODS

Ethics approval was obtained from the Sydney Children's Hospital Network Human Research Ethics Committee (reference LNR/15/SCHN/491) with a waiver for consent as no human subjects were involved, and all accessed CT studies were already deidentified. CT studies conducted previously at The Children's Hospital at Westmead (Siemens Somatom Sensation 64 slice scanner; Siemens Healthcare GmbH, Erlangen, Germany) were examined after deidentification at the source database to obtain scans with the following characteristics:

- Patient age ≤2 years;
- Reconstructed slice thickness ≤0.75 mm;
- Incorporating any section of the airway commencing from the level of the nares to the first division of the bronchial tree;
- Absent of craniofacial malformations and pathology;
- Free of upper airway distortion by endotracheal tubes, head position, or pathology in the oropharyngeal region.

A single CT dataset of the head and neck of a 21-month-old subject was identified using these criteria. This dataset was processed using Avizo Lite (FEI Software, version 9.0.1; ThermoFisher Scientific, Hillsboro, OR) via the Multi-modal Australian Sciences Imaging and Visualisation Environment (MASSIVE) where semiautomatic Hounsfield unit (HU) thresholding was used to isolate anatomical structures based on their tissue-specific attenuation ranges. These voxel-based 3D isolates were then converted into 3D polygonal meshes. For elements that could not be isolated with HU thresholding, a triple-pass, manual selection approach was used to isolate structures as they appeared in the coronal, transverse, and sagittal planes.

All meshes were then imported into Geomagic Studio 2014 (3D Systems, version 2014.0.1, Rock Hill, SC) and treated with a combination of the Quick Smooth, Defeature, and Sandpaper tools to reduce

"stair-step" artifacting (eg, a jagged surface mesh appearance from the original scan Z-axis resolution). The lasso-select and fill tools were also used to correct erroneous fusions between closely opposed parallel surfaces. When meshes were completed, the Mesh Doctor and Manifold tools were both applied to analyze and automatically correct aberrant geometry, ensuring each mesh was suitable for 3D printing.

Because the calvarium, superior orbit, pinnae and laryngeal, and tracheal cartilages were only partially captured in the original CT dataset, each required reconstruction in Geomagic with additional data. The calvarium and superior orbit were completed using the scaled-down calvarium of an adult woman, previously CT-imaged and archived in the Monash Centre for Human Anatomy Education (CHAE) collections. The pinnae were reconstructed by modifying a public domain 3D mesh available at www.thingiverse.com/thing:31843. Laryngeal and tracheal cartilages were rebuilt with a dissected adult larynx from the Monash CHAE collections, which was imaged with structured white light scanning as previously described,[19] and then scaled down in Geomagic.

Specific meshes were then modified in Geomagic to prepare them for either direct 3D printing or silicone casting and assembly. Hard tissue elements, including the cranium, mandible, and vertebrae, were articulated using silicone sleeves and inserts that were attached via interfaces carved into or molded around the osseous elements, then affixed with Smooth-On Sil-poxy silicone adhesive. Space and interfaces for the upper airway and tongue modules were also made by carving into the skeletal meshes. Molds for these and other silicone-cast parts, including the gingivae, palate, and trachea, were generated in Geomagic. Negative impressions of each part were used to make a mold cavity, which was divided in half, and pouring basins, sprues, and joinery designed in Rhinoceros (v. 5; Robert McNeel & Associates, Seattle, WA) were added to facilitate pouring and demolding.

All mold components were printed in gypsum powder using a ZPrinter 650 binder jetting 3D printer (Z Corporation, Burlington, MA). The cranium, mandible, and vertebrae were printed in White Version 3 resin, and the laryngeal and tracheal cartilages in Flexible Version 2 resin, using a Form 2 SLA printer (FormLabs, Inc, Somerset, MA). Early trials of the laryngeal cartilages and upper airway were fabricated from VeroPure White, Tango Plus, and Tango Black photopolymers, using 2 Stratasys multi-material multijet printers; the Connex 350 (Stratasys, Ltd, Rehovot, Israel; printer housed at Fuji Zerox Australia Pty Ltd, Melbourne, Australia) and the Connex 500 (Stratasys, Ltd, Rehovot, Israel; printers housed at Monash University, Department of Materials Science and Engineering, Melbourne, Australia).

All silicone elements were cast with Smooth-On (Smooth-On, Inc, Macungie, PA) addition-cured, platinum-catalyzed silicones "Ecoflex 00-30" and "Ecoflex 00-10." Smooth-On Silc Pig pigment was added at a concentration of 0.001%–3%, and combinations of Pantone 488C (flesh tone), White C, 107C (yellow), and 7421C (blood) to emulate different soft-tissue types. The silicone was then depressurized in approximately 1 bar vacuum chamber to remove excess air and poured into 3D-printed gypsum molds, which were primed with Mann-Release Ease Release 200 (Smooth-On, Inc, Macungie, PA) and whose seams were plugged with oil-based modeling clay. The silicone was then cured at room temperature (21 °C) for approximately 16 hours. After demolding each component, any flashing was trimmed with scissors, and small holes or defects were filled with Sil-poxy.

After the production of the initial simulator components, a process of staged prototype production was undertaken with qualitative feedback provided by the clinical investigators regarding generated tissue characteristics and desirable features of developed models. Key priorities for the overall model design included anatomical fidelity, haptic qualities, realistic movements, and the ability to replace individual components of the model to allow cleaning, maintenance, or modification.

RESULTS

Trial of Multijet Manufacturing

Initial structured light imaging data of the pharynx, larynx, and trachea was utilized to produce a series of photopolymer-based, embedded laryngeal cartilages with varying tissue characteristics (expressed as shore hardness). Although anatomical features were accurate, tissue characteristics changed with time (likely due to progressive ultraviolet [UV] exposure), and the overall shore hardness achieved was inconsistent with the tissue being stimulated. This approach to component production was not pursued after initial trials.

Material Analogs

Gypsum-powder infiltration prints were suitable analogs for bone but as bone drilling or other osteological procedures were not part of the use of this model, it was determined that osseous elements with high shore hardness could be produced using an acrylonitrile butadiene styrene (ABS) or VeroPure White (photopolymer) material. It was also determined that the soft tissues of the tongue, skin, vertebral column, neck muscle and upper airway, and oral mucosa modules should be replicated using castable silicones (Ecoflex 00-10 and 00-30) then colored with Silc Pig silicone pigment. Several photopolymer combinations were assessed for their haptic similarities to pediatric tracheal cartilages, and it was determined that FLX9760, with a shore hardness of 60, was the most suitable material.

Prototype 1

To achieve functional simulation of the pediatric airway, we initially divided the segmented anatomical structures into a series of discrete interlocking modules. This allowed independent customization of each module's material properties, improved mechanical interfacing to facilitate realistic movement, and rapid changes in the structure of the overall prototype. Osseous tissues (cranium, mandible, and cervical vertebrae) were printed separately. The cranium and cervical vertebrae modules were united with a molded silicone insert that simulated the axial connective tissue and nervous tissue within the vertebral canal (Figure 1A). The second, cervical fascia and muscle module, represented the combined cervical epaxial and hypaxial fascia, musculature, and nonrespiratory viscera; it aimed to provide a distal anchor point for other modules (Figure 1B). The third module consisted of the mandible, which interfaced with the tongue module (Figure 1C) and inserted into a companion infratemporal region soft tissue module, which provided a mechanical bridge to the basicranium, replicating the temporomandibular joint (TMJ). The fourth module of an isolated tongue with surrounding oropharyngeal soft tissue was designed to interlock with the mandible module (Figure 1D). The fifth module combined all soft-tissue components of the palate, oral cavity mucosa, nasopharyngeal and laryngeal tracts, and the esophagus, and was designed to attach to the mandible and maxilla and insert into the nasal cavity simultaneously (Figure 1E). Finally, a sixth "skin" module was constructed for the superficial tissues, including epidermis, dermis, and any deeper musculature or fascia not already included.

The first module, which united the cranium and vertebral column, proved simple and effective and was carried through all subsequent design iterations, and the second module anchored the others sufficiently. However, the T-pin interface between the tongue and the mandible (Figure 1C) proved unstable and was subsequently removed from both modules, and the tongue was redesigned to fit within the first iteration of the upper airway module. To insert the upper airway module into the cranium without damage, it became clear that several anatomical features needed to be compromised, and in subsequent prototypes, an open channel was digitally cut between the foramen magnum and the nasal cavity of the cranial module to facilitate assembly and disassembly. Additionally, the Tango Black photopolymer used for the upper airway module was an inappropriate color and texture and became stiff and brittle after repeated use. The revised tongue insert was difficult to deform, prompting a further revision of the glossomandibular interface. Finally, the skin module's surface set rough and tacky, which impeded assembly, and its thickness, combined with the stiff oral component of the upper airway, imparted excessive resistance to mandibular depression.

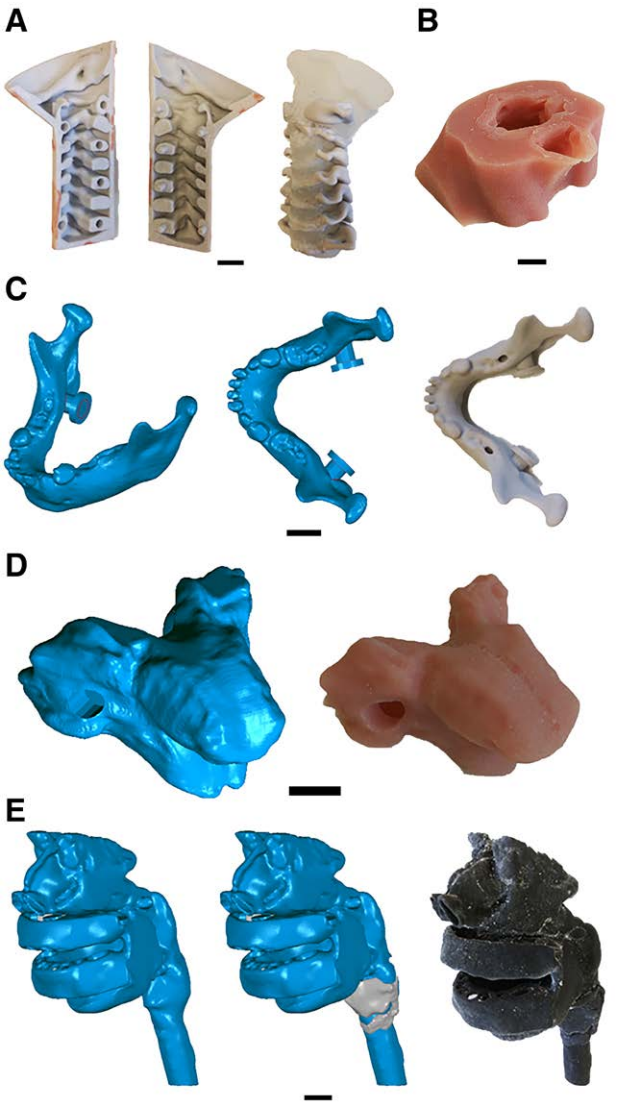

Figure 1. Examples of simulator components developed for prototype 1. A, Two-part 3D-printed mold (Z650 powder print) for casting the vertebral column insert with Ecoflex 00-30 alongside an anterior oblique view of the cast silicone insert with individual 3D-printed (Z650 powder print) vertebrae; (B) superior oblique view of the cast cervical fascia and muscle module in Ecoflex 00-10; (C) superior oblique and superior view screenshots and 3D-printed (Z650 powder print) mandible with T-pin anchor points for attaching silicone cast oral cavity and tongue components; (D) anterior oblique screenshot and cast silicone tongue module in Ecoflex 00-10 with reciprocal pin recesses for the mandible anchor points; (E) anterior oblique screenshots and 3D-printed (Connex 350 multi-material) combined upper airway, gingivae, and oral mucosa in Tango Black material with embedded tracheal cartilages. Scale bars = 1 cm. 3D indicates 3-dimensional.

Prototype 2

To simplify the upper airway module and address difficulties with its oral components, the oral cavity was extensively redesigned. The new glossomandibular

interface consisted of an arching T-shaped groove along the sublingual foveae of the mandible module, which accepted a corresponding arching T-shaped protrusion from the sublingual region of the tongue module (Figure 2A). Most of the oral mucosa was replaced with 3-mm-thick cast-silicone overlays that attached to the mandible and maxilla by truncated conical pins and included the uvula and hard and soft palates but excluded the floor of the mouth (Figure 2B). The lateral oropharyngeal walls and the retromolar trigones were reproduced by altering the TMJ sleeves (Figure 2C). The revised upper airway module had open fauces, which attached to the new tongue module via a serrated mortise and tenon joint, and was printed in Tango Plus photopolymer (Figure 2D).

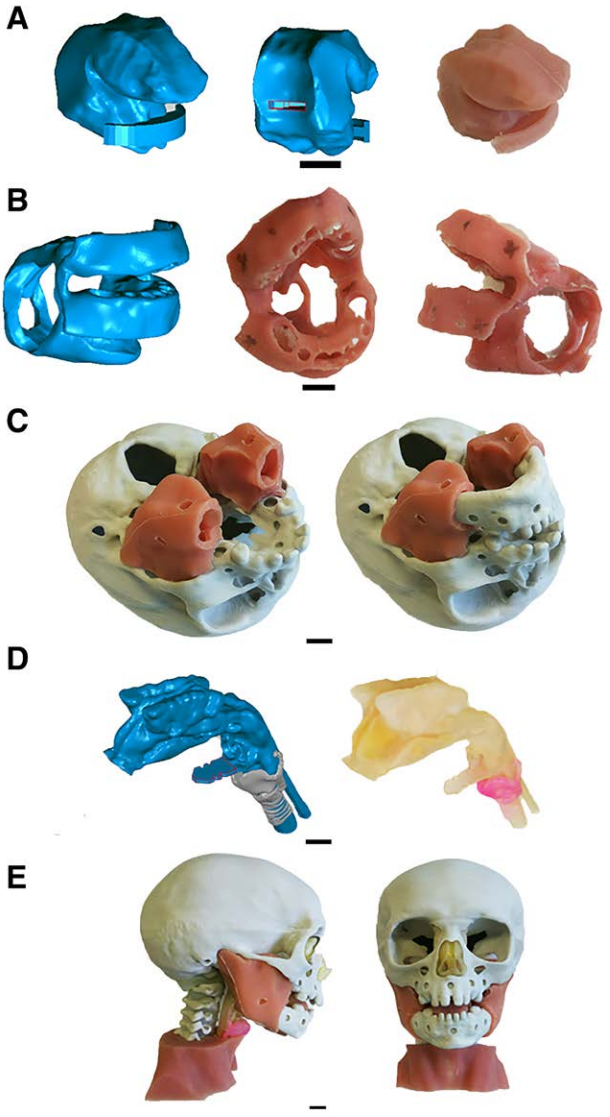

Figure 2. Examples of simulator components developed or adapted for prototype 2. A, Anterior oblique screenshots and cast silicone tongue module in Ecoflex 00-10 with redesigned mortise-and-tenon for joining the posterior aspect with the pharyngeal component, and a T-shaped groove for joining the mandible; (B) anterior oblique screenshot and cast silicone oral mucosal module in Ecoflex 00-10; (C) inferior oblique view of the cast silicone temporomandibular sleeves in Ecoflex 00-10 affixed to the 3D-printed (Z650 powder print) skull with and without the 3D-printed (Z650 powder print) mandible in position; (D) anterior oblique screenshot and view of the 3D-printed (Connex 350 multi-material) revised nasopharyngeal model in Tango Clear material with tenon for tongue articulation and embedded tracheal cartilages; (E) lateral and anterior view of the assembled prototype 2 simulator (without overlying skin or oral mucosa modules) to demonstrate the fit of skeletal, muscular, TMJ, and nasopharyngeal components. Scale bars = 1 cm. 3D indicates 3-dimensional; TMJ, temporomandibular joint.

This assembly had a more depressible mandible due to the increased modularity of the oral components (Figure 2E); however, the skin component still imparted considerable resistance, the increased modularity decreased the cohesion of the assembled model, causing the upper airway module to periodically detach from the tongue module, and the thinness of the gingivae modules meant that pour-casting outcomes were inconsistent. Additionally, despite being a more representative color, the Tango Plus upper airway continued to suffer from brittleness and haptic inaccuracy.

Prototype 3

The third prototype incorporates further evolution in the materials used (Tables 1 and 2). In the third prototype, modifications were made to the gingivae (Figure 3A), upper airway (Figure 3B), skin, and tongue modules. The gingivae molds were thickened to improve casting outcomes, and the tongue module was hollowed out to allow for it to be filled with a more deformable hydrogel material (Ballistics Gel, Clear Ballistics, Fort Smith, AR) (Figure 3A). To achieve more appropriate material properties for the upper airway, the module was cast in Ecoflex 00-30 (Figure 3B). The external nares and fauces of this module were then made patent before assembly by excising the overlying silicon. Finally, to address the tacky, inflexible skin, its thickest parts, the cheeks, were reduced, and Slide Surface Tension Diffuser was added to produce a smoother surface (Figure 3C, D).

DISCUSSION

The described process of developing multiple modern fabrication techniques for a pediatric airway model produces more realistic models for procedural training. Combining patient imaging data with computer-aided design allows precision in constructing anatomical modules. The current range of commercially available 3D printers and printable materials imposes restrictions on the range of material properties that can be directly manufactured; this particularly impacts producing anatomical modules with low shore hardnesses that mimic human tissue properties. As demonstrated here, the production of replicas integrating multiple tissues is best achieved

Table 1. A Summary Table of Materials Used to Fabricate Each Module in Each of the 3 Prototype Iterations

Materials	FormLabs resin	Ecoflex 00-10	Ecoflex 00-30	Tango Black	Tango Plus	FLX 9760
Prototype 1	Mandible Cranium	Tongue Neck muscle	Skin Vertebral column Temporomandibular sleeve	Combined upper airway, gingivae and oral mucosa	n/a	Laryngeal and tracheal cartilages
Prototype 2	Mandible Cranium	Tongue Neck muscle Gingivae Temporomandibular sleeve	Skin Vertebral column Temporomandibular sleeve	n/a	Upper airway	Laryngeal and tracheal cartilages
Prototype 3	Mandible Cranium Tracheal cartilages	Gingivae Temporomandibular sleeve	Skin Vertebral column Temporomandibular sleeve Upper airway	n/a	n/a	n/a

Table 2. A Summary Table of Prototype 3 Modules, Materials, and Hardware Used to Fabricate Each Module

Modules	Data source and capture method	Fabrication method	Material	Pigment
Laryngeal cartilages	Prosected adult larynx with Artec Spider structured light scanner	FormLabs Form 2 SLA printer	FormLabs flexible photoreactive resin (FL-RS-F2-FLGR-02)	None
Cranium Mandible Vertebrae	21-month-old CT neck with Somatom sensation 64-slice CT		FormLabs rigid photoreactive resin (RS-F2-RGWH-01)	White
Neck insert Upper gingivae[a] Lower gingivae[a] Temporomandibular joint sleeves[a] Tongue Airway		Silicone casting with 3D-printed molds	Ecoflex 00-10 Ecoflex 00-10 Silicone Thinner (5wt%) Ecoflex 00-30 Silicone Thinner (5wt%)	Flesh and blood
Vertebral column[a]			DragonSkin 10 Fast	None
Skin			Ecoflex 00-30 Slide Surface Tension Diffuser (1.5wt%)	Flesh

Abbreviations: 3D, 3-dimensional; CT, computerized tomography; SLA, stereolithography.
[a]These are bespoke modules, not segmented from CT data.

by combining conventional molding techniques and materials with more modern 3D printing technology. The most recent prototype displays anatomy and functionality with a good haptic response (see Supplemental Digital Content 1, Video, http://links.lww.com/AA/D223, for an overview of the features of Prototype 3).

VIDEO+

The potential for fabrication methods, such as 3D printing, to contribute to a variety of applications, such as anatomical education, surgical planning, production of surgical implants, and development of skills training model, has been discussed elsewhere.[15–17,20] The multifaceted approach we describe offers immediate advantages for education and skills training, as well as the assessment of medical equipment and techniques. Even recent publications describing 3D-printed pediatric airway models with positive ratings of simulator fidelity highlighted issues with tissue resistance and lack of neck mobility.[21] Our study represents a further advance by combining techniques to enhance fidelity. As a wider range of materials becomes available, further evolution of this approach will follow.[22,23]

While model refinement is an ongoing process, the produced prototypes already offer an option to conduct research in areas highly relevant to pediatric airway management. One example is a further exploration of front-of-neck access techniques for the "can't intubate, can't oxygenate" situation. While rare, this is a potentially fatal complication of pediatric airway management.[24] In developing guidelines for the management of the difficult pediatric airway, a consensus approach to this situation in patients under the age of 8 proved difficult due to a relative paucity of evidence.[25] Available animal models, including white rabbits and pigs, do not replicate real patient anatomy.[26–29] There have been other efforts to produce front-of-neck models for pediatric training, but anatomical fidelity continues to be sacrificed to meet design goals such as simplicity of reproduction.[30]

Our prototype shows that pediatric airway models need not compromise on anatomical and functional fidelity. Development of mannequins with accurate anatomy and haptic feedback offers a useful model to research the applicability of different front-of-neck access techniques or test devices to ascertain if they are fit for purpose.[31] Development of evidence-based guidelines requires this capability to evaluate whether techniques are physically feasible in pediatric patients and performed effectively by clinicians. Potential

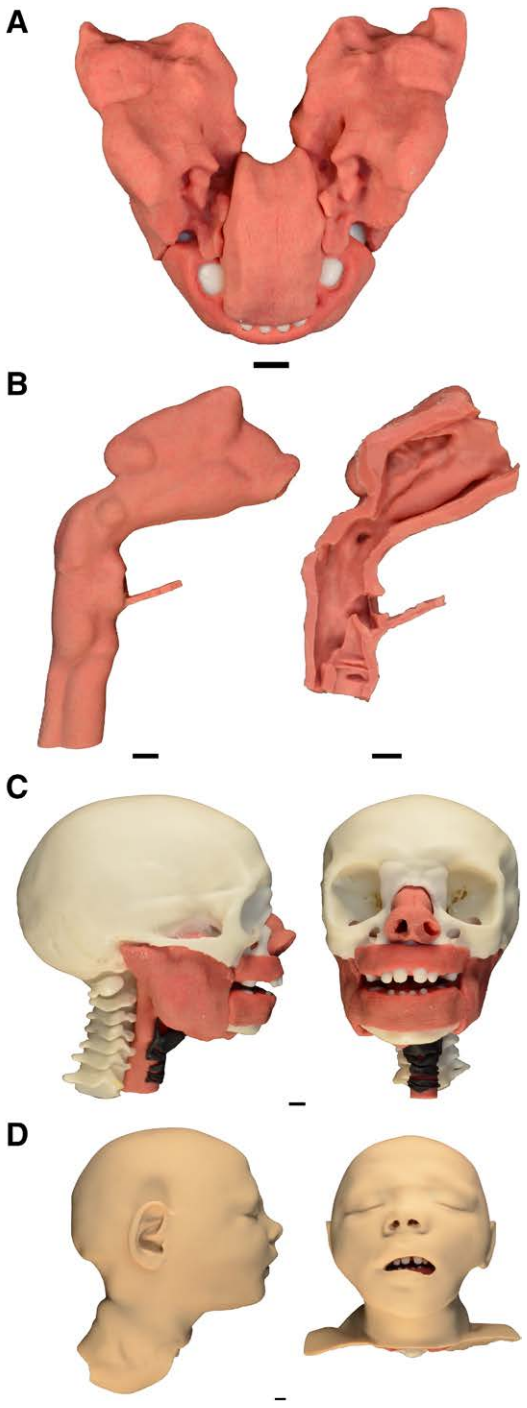

Figure 3. Examples of simulator components developed or adapted for prototype 3. A, Superior view of the cast silicone Ecoflex 00-10 tongue, mandibular gingivae, and Ecoflex 00-30 temporomandibular sleeves in articulation with the 3D-printed (Form 2 SLA White resin) mandible; (B) lateral view of the cast silicone Ecoflex 00-30 nasopharyngeal module with midsagittal section demonstrating the reproduction of internal anatomical structures from the conchae and auditory tube meatus to the mucosal folds of the epiglottis and larynx; (C) lateral and anterior view of the assembled prototype 3 simulator with the cast silicone nasopharynx module, gingivae, tongue, and temporomandibular sleeves with the 3D-printed (Form 2 SLA White resin) skull, mandible, and vertebral column modules; (D), lateral and anterior views of the fully assembled prototype 3 with cast Ecoflex 00-30 skin and superficial fascia. Scale bars = 1 cm. 3D indicates 3-dimensional; SLA, stereolithography.

complication rates, such as posterior tracheal injury, also require consideration. The ability to replace individual components of the model would allow repeated testing of techniques, rather than being limited by available animal models. As our approach supports the generation of models for different ages and with the capability to modify individual components, evaluation of techniques can be broadened across different patient ages or pathologies.

The adaptability of this mannequin is one of its greatest strengths. The same model could be utilized to support the development of a range of skills such as bag-mask technique, supraglottic airway insertion, laryngoscopy and intubation, and then front-of-neck access techniques with only individual components requiring replacement if they are damaged during the process. Reproduction of pathology is already being used in surgical planning but could be applied to broader education initiatives.[32,33] With the same basic model architecture, a variety of conditions known to be associated with difficult airway management can be reproduced, and the full range of airway techniques can then be practiced in all of them. This mannequin will continue to be refined to allow adaptation to reproduce micrognathia (as in Pierre-Robin sequence), midface changes (eg, those of Treacher-Collins), or tracheal or laryngeal lesions.[14]

Understandable questions that arise regarding this mannequin are the costs in materials and labor involved. The relative direct production costs of the 3D printed and silicone components for our final prototype, including the reusable molds used in the production process, are relatively modest (Supplemental Digital Content 2, Table 1, http://links.lww.com/AA/D224). Our group utilized pre-existing 3D printing and materials casting research infrastructure, which facilitated the iterative design process to generate the final components described here. Any statement of the number of hours of labor involved in the development of this prototype can only be an estimate. Hours were invested in early prototypes that—while not reflected in the final models—nonetheless contributed toward the final design. Collectively, we estimate the project involved about 380 hours of segmentation, iterative digital component and mold design, and physical printing and casting. Less than 10% of those hours would now reflect the time required to transition all the digital files from 1 "version set" to production of a complete prototype. Minor adjustments to a single module (eg, the tongue, the mandible) can easily be completed within a few hours.

There remain limitations to this method of producing airway mannequins. The models do not replicate other situations that may challenge airway management, such as bleeding or excessive secretions. However, this sort of fidelity is not presently supported by more

traditional models. The same applies to the inability to produce changes in clinical appearance, such as cyanosis, erythema, or pallor. At this stage of development, the mannequins are not matched-up to the lower airways or representative lung fields. This progression will be required to assist in replication of the subjective experience of bag-mask ventilation or ventilation via other means but is something readily developed through adaptations of the existing model components. The next critical step is to assess the performance of our pediatric airway simulator within an educational environment as previously done with newly developed 3D-printed educational tools and simulators.[15,16,34,35] Data gathered from experienced and novice practitioners comparing and contrasting the performance of our prototype alongside other airway simulators will allow for evaluation of the performance of this model in the context of both pediatric airway education and research into specific airway management techniques.

CONCLUSIONS

Existing 3D printing technology alone does not currently make it possible to reproduce the dynamic range or haptic properties necessary to mimic realistic pediatric airway behavior. The approach described in this study, by breaking down the anatomical components into discrete printable elements, allowed us to generate models in which individual tissue characteristics could be mimicked more closely that a single plastic or rubber. This results in mannequins with high degrees of physical and functional fidelity. While there will be further refinement of this approach, the general principles are directly applicable to the generation of other anatomically appropriate models suitable for other areas of anesthesia research and education.

ACKNOWLEDGMENTS

The authors acknowledge the help of Rachel Fitzpatrick in identifying appropriate scans from the database, and Rain Gidley of Rain Gidley Studios (Melbourne) for his assistance in producing cast prototype components featured in the publication. The authors would also like to acknowledge the assistance of Dr Mark Lovell and Caleb Lapointe in the production of the accompanying Supplemental Digital Content 1, Video, http://links.lww.com/AA/D223.

VIDEO+

DISCLOSURES

Name: Andrew D. Weatherall, BMed.
Contribution: This author helped conceive the study, provide the data, test prototype simulators, and write and edit the manuscript.
Name: Matthew D. Rogerson, BSc Hons.
Contribution: This author helped segment radiographic data, edit mesh, develop and produce the prototype, and produce and edit the manuscript.
Name: Michelle R. Quayle, BSc Hons.
Contribution: This author helped supervise the segmentation, edit mesh, construct model components, and edit the manuscript.
Name: Michael G. Cooper, MBBS.
Contribution: This author helped conceive the study, provide the data, test prototype simulators, and edit the manuscript.
Name: Paul G. McMenamin, PhD.
Contribution: This author helped conceive the study, execute methods, and edit the manuscript.
Name: Justin W. Adams, PhD.
Contribution: This author helped formulate and supervise all research presented here from idea conception to execution, including manuscript writing and editing.
This manuscript was handled by: James A. DiNardo, MD, FAAP.

REFERENCES

1. Fiadjoe JE, Nishisaki A, Jagannathan N, et al. Airway management complications in children with difficult tracheal intubation from the pediatric difficult intubation (PeDI) registry: a prospective cohort analysis. *Lancet Respir Med.* 2016;4:37–48.
2. Heinrich S, Birkholz T, Ihmsen H, Irouschek A, Ackermann A, Schmidt J. Incidence and predictors of difficult laryngoscopy in 11,219 pediatric anesthesia procedures. *Paediatr Anaesth.* 2012;22:729–736.
3. Belanger J, Kossick M. Methods of identifying and managing the difficult airway in the pediatric population. *AANA J.* 2015;83:35–41.
4. Engelhardt T, Virag K, Veyckemans F, Habre W; APRICOT Group of the European Society of Anaesthesiology Clinical Trial Network. Airway management in paediatric anaesthesia in Europe-insights from APRICOT (anaesthesia practice in children observational trial): a prospective multicentre observational study in 261 hospitals in Europe. *Br J Anaesth.* 2018;121:66–75.
5. Cook TM, Woodall N, Frerk C; Fourth National Audit Project. Major complications of airway management in the UK: results of the fourth National audit project of the Royal College of Anaesthetists and the difficult airway society. Part 1: anaesthesia. *Br J Anaesth.* 2011;106:617–631.
6. Schleelein LE, Vincent AM, Jawad AF, et al. Pediatric perioperative adverse events requiring rapid response: a retrospective case-control study. *Paediatr Anaesth.* 2016;26:734–741.
7. Litman RS, Weissend EE, Shibata D, Westesson PL. Developmental changes of laryngeal dimensions in unparalyzed, sedated children. *Anesthesiology.* 2003;98:41–45.
8. Wani TM, Bissonnette B, Rafiq Malik M, et al. Age-based analysis of pediatric upper airway dimensions using computed tomography imaging. *Pediatr Pulmonol.* 2016;51:267–271.
9. Wani TM, Rafiq M, Akhter N, AlGhamdi FS, Tobias JD. Upper airway in infants-a computed tomography-based analysis. *Paediatr Anaesth.* 2017;27:501–505.
10. Sunder RA, Haile DT, Farrell PT, Sharma A. Pediatric airway management: current practices and future directions. *Paediatr Anaesth.* 2012;22:1008–1015.
11. Schebesta K, Hüpfl M, Rössler B, Ringl H, Müller MP, Kimberger O. Degrees of reality: airway anatomy of high-fidelity human patient simulators and airway trainers. *Anesthesiology.* 2012;116:1204–1209.
12. Schebesta K, Hüpfl M, Ringl H, Machata AM, Chiari A, Kimberger O. A comparison of paediatric airway anatomy with the SimBaby high-fidelity patient simulator. *Resuscitation.* 2011;82:468–472.
13. Sawyer T, Strandjord TP, Johnson K, Low D. Neonatal airway simulators, how good are they? A comparative study of physical and functional fidelity. *J Perinatol.* 2016;36:151–156.

14. Sheeran PW, Walsh BK, Finley AM, Martin AK, Brenski AC. Management of difficult airway patients and the use of a difficult airway registry at a tertiary care pediatric hospital. *Paediatr Anaesth.* 2014;24:819–824.
15. Adams JW, Paxton L, Dawes K, Burlak K, Quayle M, McMenamin PG. 3D printed reproductions of orbital dissections: a novel mode of visualising anatomy for trainees in ophthalmology or optometry. *Br J Ophthalmol.* 2015;99: 1162–1167.
16. McMenamin PG, Quayle MR, McHenry CR, Adams JW. The production of anatomical teaching resources using three-dimensional (3D) printing technology. *Anat Sci Educ.* 2014;7:479–486.
17. Chae MP, Rozen WM, McMenamin PG, Findlay MW, Spychal RT, Hunter-Smith DJ. Emerging applications of bedside 3D printing in plastic surgery. *Front Surg.* 2015;2:25.
18. Chao I, Young J, Coles-Black J, Chuen J, Weinberg L, Rachbuch C. The application of three-dimensional printing technology in anaesthesia: a systematic review. *Anaesthesia.* 2017;72:641–650.
19. Adams JW, Olah A, McCurry MR, Potze S. Surface model and tomographic archive of fossil primate and other mammal holotype and paratype specimens of the ditsong national museum of natural history, Pretoria, South Africa. *PLoS One.* 2015;10:e0139800.
20. Smith ML, Jones JFX. Dual-extrusion 3D printing of anatomical models for education. *Anat Sci Educ.* 2018;11:65–72.
21. Kovatch KJ, Powell AR, Green K, et al. Development and multidisciplinary preliminary validation of a 3-dimensional-printed pediatric airway model for emergency airway front-of-neck access procedures. *Anesth Analg.* 2020;130:445–451.
22. Ravi P, Wright J, Shiakolas PS, Welch TR. Three-dimensional printing of poly(glycerol sebacate fumarate) gadodiamide-poly(ethylene glycol) diacrylate structures and characterization of mechanical properties for soft tissue applications. 2019;107:664–671.
23. Shin DS, Kang SH, Kim KH, et al. Development of a deformable lung phantom with 3D-printed flexible airways. *Med Phys.* 2020;47:898–908.
24. Santoro AS, Cooper MG, Cheng A. Failed intubation and failed oxygenation in a child. *Anaesth Intensive Care.* 2012;40:1056–1058.
25. Black AE, Flynn PE, Smith HL, Thomas ML, Wilkinson KA; Association of Pediatric Anaesthetists of Great Britain and Ireland. Development of a guideline for the management of the unanticipated difficult airway in pediatric practice. *Paediatr Anaesth.* 2015;25:346–362.
26. Prunty SL, Aranda-Palacios A, Heard AM, et al. The "can't intubate can't oxygenate" scenario in pediatric anesthesia: a comparison of the Melker cricothyroidotomy kit with a scalpel bougie technique. *Pediatr Anesth.* 2014;25:400–4.
27. Stacey J, Heard AMB, Chapman G, et al. The "can't intubate can't oxygenate" scenario in pediatric anesthesia: a comparison of different devices for needle cricothyroidotomy. *Pediatr Anesth.* 2012;22:1155–1158.
28. Johansen K, Holm-Knudsen RJ, Charabi B, Kristensen MS, Rasmussen LS. Cannot ventilate-cannot intubate an infant: surgical tracheotomy or transtracheal cannula? *Paediatr Anaesth.* 2010;20:987–993.
29. Holm-Knudsen RJ, Rasmussen LS, Charabi B, Bøttger M, Kristensen MS. Emergency airway access in children - transtracheal cannulas and tracheotomy assessed in a porcine model. *Pediatr Anesth.* 2012;22:1159–1165.
30. Doucet G, Ryan S, Bartellas M, Parsons M, Dubrowski A, Renouf T. Modelling and manufacturing of a 3D printed trachea for cricothyroidotomy simulation. *Cureus.* 2017;9:e1575.
31. Coté CJ, Hartnick CJ. Pediatric transtracheal and cricothyrotomy airway devices for emergency use: which are appropriate for infants and children? *Paediatr Anaesth.* 2009;19(suppl 1):66–76.
32. Reighard CL, Green K, Powell AR, Rooney DM, Zopf DA. Development of a high fidelity subglottic stenosis simulator for laryngotracheal reconstruction rehearsal using 3D printing. *Int J Pediatr Otorhinolaryngol.* 2019;124:134–138.
33. Stramiello JA, Saddawi-Konefka R, Ryan J, Brigger MT. The role of 3D printing in pediatric airway obstruction - a systematic review. *Int J of Pediatr Otorhinolaryngol.* 2020;132: 109923.
34. Nagassa RG, McMenamin PG, Adams JW, Quayle MR, Rosenfeld JV. Advanced 3D printed model of middle cerebral artery aneurysms for neurosurgery simulation. *3D Print Med.* 2019;5:11.
35. Lim KH, Loo ZY, Goldie SJ, Adams JW, McMenamin PG. Use of 3D printed models in medical education: a randomized control trial comparing 3D prints versus cadaveric materials for learning external cardiac anatomy. *Anat Sci Educ.* 2016;9:213–221.